

Multi-modal Study of Angular Momentum Distribution of Fission Fragments as a Result of Bending Modes

İ. Özkan,^a Z. Büyükmumcu,^b H. Sökmen,^a and M. Kildir^{*,a}

^aDepartment of Chemistry, Middle East Technical University, 06531 Ankara, Turkey

^bDepartment of Chemistry, Erciyes University, 38039 Kayseri, Turkey

Received: November 13, 2001; In Final Form: November 13, 2001

The average angular momentum of the primary fission fragments as a function of their masses was calculated using the wave function of the bending mode excitation at the scission point. The scission configuration was assumed to be determined by the pre-scission shapes of fissioning nucleus within the multimodal fission model. Results in $^{235}\text{U}(n_{\text{th}}, f)$ is in good agreement with the recent experimental data.

1. Introduction

The average angular momentum of the fission fragments as a function of their masses is determined for various nuclei with the study of prompt γ rays.^{1–5} The recent observations of γ rays are carried out with multi-fold γ -ray coincidences between several detectors of Compton suppressed Ge arrays.

A model for calculating the angular momentum distribution of fission fragments was proposed by Rasmussen et al.⁶ in which a scission point approximation of a spheroid tangent to a sphere was made. The average angular momentum of fragment ^{108}Ru as $\sim 6\hbar$ is calculated in $^{239}\text{Pu}(n_{\text{th}}, f)$. The model was generalized for the case when both fragments were deformed by Pfabe and Dietrich^{7,8} and numerical calculations for the even-even fragments of $^{235}\text{U}(n_{\text{th}}, f)$ were carried out. Recently, Rasmussen et al.⁹ have calculated the increase in angular momentum due to Coulomb excitation for ^{104}Mo formed in the cold fission of $^{252}\text{Cf}(\text{sf})$. The small spin observed for ^{104}Mo , $3.8\hbar$, implies that the primary fission fragment may have no spin at the scission point.

In this study, the average angular momentum of the primary fission fragments as a function of their masses were calculated using the wave function of the wriggling-bending motion at the scission point. The pre-scission shapes were determined by the experimental mass and kinetic energy distributions. The neutron multiplicity distribution was well accounted by these shapes.

2. Calculations

2.1. Determination of Pre-scission Shape Parameters. According to the BGM model,¹⁰ after leaving the compound or ground state, the nucleus could split into fragments by a number of paths, referred as *modes*. These paths are categorized as standard 1 (S1), standard 2 (S2), and superlong (SL). Each mode is characterized by the shape parameters of the fissioning nucleus at the scission point. A fissioning nucleus in a given mode can be represented by pre-scission shape of a fairly long flat neck connecting two relatively large heads. Parameters of this representation are the semi-length (l), the neck radius where the neck is thinnest (r), the thinnest position of the neck (z), the curvature (c), and the extension of the neck (a), the transitional points (ζ_1 and ζ_2), and the radii of spherical heads (r_1 and r_2). Parameters for each mode of fissioning system have been determined by recipes given in References 10, 11.

2.2. Calculation of Angular Momentum of Fission Fragments. In order to calculate the angular momentum distribution of fission fragments, a model, first proposed by Rasmussen et al.,⁶ and later extended to the deformed complementary fission fragments by Pfabe and Dietrich,^{7,8} was followed. The

coordinate systems and parameters involved in our study are depicted in Figure 1. The nucleus was assumed to decay into primary fission fragments. They were modeled by embedded ellipsoids with major, a_i and minor axes, b_i . These ellipsoids separated by a center-center distance, σ , interact through the Coulomb potential¹² and nuclear potential¹³ so that the total potential energy of the system is the sum of these two potentials. The total potential energy was calculated for each complementary pair as a function of distance between the centers for their aligned configuration. Our results showed that the minimum potential energy occurs at a distance of $\sigma \approx a_1 + a_2$. All angular momentum calculations reported in this work were done at the minimum potential energy. The kinetic energy associated with the relative motion of nascent fragments was obtained with the adiabatic approximation. Ignoring the coupling between the internal and total angular momentum together with rotation of fragments around their symmetry axes, the Hamiltonian describing the internal motion became,

$$H = \frac{l_1 \cdot l_2}{\mathfrak{I}_0} + \frac{l_1^2}{2B_1} + \frac{l_2^2}{2B_2} + C_1 \sin^2 \theta_1 + C_2 \sin^2 \theta_2 - C_{12} \sin \theta_1 \sin \theta_2 \cos(\phi_2 - \phi_1), \quad (1)$$

where l_i is the angular momentum of the i -th fragment about its center of mass, $\mathfrak{I}_0 = \mu\sigma^2$, with μ being the reduced mass of the two fragments and σ being center-to-center distance (Figure 1), B_1 and B_2 are the reduced inertias, C_1 , C_2 , and C_{12} are coefficients calculated depending on shape and charge of fragments. Angles θ_1 , θ_2 , ϕ_1 , and ϕ_2 are defined in Figure 1. We solved the Schrödinger equation exactly. First we obtained a suitable basis set by solving one particle eigenvalue equations. We then used these functions as a product-bases for expanding the two-fragment eigenfunctions. Due to the factorization provided by the M quantum number and the even-odd parity of state functions, the problem was amendable to practically exact solutions. The average values of l_1 and l_2 quantum numbers for two fragments were evaluated with the calculated wave functions. For non-zero temperatures, they were obtained with Boltzmann averaging.

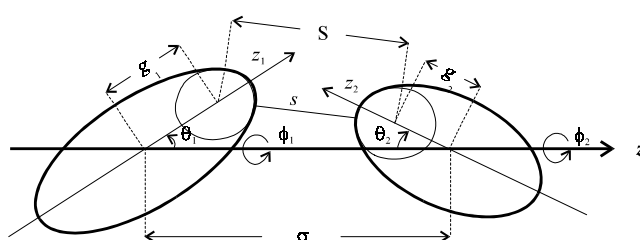


Figure 1. The coordinate systems and definition of parameters.

*Corresponding author. E-mail: kildir@metu.edu.tr. FAX: +90-0312-210-1280.

TABLE 1: The precission shape parameters for three low-energy fissioning systems.

	l / fm	r / fm	c / fm ⁻¹	Z / fm	r_1 / fm	r_2 / fm	ζ_1 / fm	ζ_2 / fm	a / fm	Weight / %
²³⁵U(n_{th}, f)										
Standard 1	15.00	2.73	0.01	0.63	6.04	5.50	4.71	14.36	0.86	17.92
Standard 2	16.30	2.96	0.0053	1.08	6.01	5.14	4.30	18.18	1.23	81.98
Superlong	18.90	3.39	0.01	0.00	4.88	4.88	1.38	26.66	5.17	0.09
²⁴⁸Cm(sf)										
Standard 1	16.20	2.95	0.038	0.43	5.85	5.54	3.39	17.91	2.76	10.50
Standard 2	17.10	3.11	0.0060	0.78	5.89	5.30	3.84	19.69	1.55	55.50
Standard 3	18.10	3.29	0.0070	1.44	5.76	4.87	3.35	23.06	2.56	26.00
Superlong	20.80	3.30	0.011	0.00	4.71	4.71	0.87	31.32	80.00	0.25
²⁵²Cf(sf)										
Standard 1	16.60	2.25	0.0011	0.37	6.12	5.78	5.15	16.51	0.69	14.45
Standard 2	17.37	2.50	0.0030	0.71	6.14	5.53	4.80	18.95	1.07	46.60
Standard 3	19.10	3.47	0.0069	1.50	5.43	4.67	2.16	26.78	3.68	37.79
Superlong	19.50	3.00	0.0025	0.00	5.47	5.47	3.27	24.79	1.87	1.22

3. Results and Discussion

The shape parameters together with fission mode probabilities were determined for ²³⁵U(n_{th}, f), ²⁴⁸Cm(sf), and ²⁵²Cf(sf) and they are given in Table 1. The radius parameter $r_0 = 1.2249$ fm was used throughout the calculations. The determined shapes were used to calculate many experimentally measurable quantities in fission using the Monte-Carlo Method. The results of these calculations and their comparison with the experimental results will be published in the forthcoming paper.

The model described in sect. 2.2 was used to calculate the average angular momenta of complementary even-even primary fission fragments for ²³⁵U(n_{th}, f), ²⁴⁸Cm(sf), and ²⁵²Cf(sf). The deformation parameters of fragments at scission were obtained by using the precission shape of each mode. The prompt neutron multiplicity as a function of fission fragment masses was calculated for each system. The close correlation between the calculated results and the experimental data for prompt neutron multiplicity gave a strong support to the correctness of the shapes employed in this study. The even- Z even- A complementary primary fragments with the largest independent yields in their corresponding mass chains according to the Z_p model¹⁴ were chosen for angular momentum calculations as long as their isobaric mode probabilities were larger than 1%. The total potential energy taken as the sum of the shape dependent Coulomb and Proximity Potentials was calculated for each fragment pair as a function of the distance between the centers for their aligned configuration. It has been seen that the extremum points of the potential energy curves move to a larger center-center distances as one goes from S1 to S2 and then to SL mode. It has also been observed that there is a decrease in the potential energy in the same order. Both of these observations are consistent with the formation of more deformed fragments in this order. We assume that the distribution of angular momenta between the complementary fragments is determined in the scission valley, and not seriously altered during the rapid passage through the low scission barrier.

The average angular momenta of the primary fission fragments as a function of their mass numbers were calculated in the various fission modes of all fissioning systems. The results for ²³⁵U(n_{th}, f) are shown in Figure 2 together with their weighted average over these modes. Angular distribution of the γ ray emitted by the fragments¹⁵ shows that the direction of angular momentum is perpendicular to the fission axis in accordance with our results. The trend of angular momentum values for each mode is very similar to that of the average neutron multiplicity values since both of them are directly related to the deformation of fragments at the scission point. It is seen from Figure 2 that in each mode, the angular momenta smoothly increase as a function of the fragment mass. This property of the angu-

lar momenta is closely related to a similar trend in the restoring force constants (C_i) and the reduced moment of inertia (B_i). Ignoring the coupling between the two fragments, and making the harmonic approximation, it may be shown semiclassically⁸ that the ground state angular momentum of a fragment is proportional to $(C_i B_i)^{1/4}$. Thus, the change in the angular momenta parallels those in C_i and B_i . The sharp decrease in the average angular momentum around the symmetric division is related to the asymmetric precission shapes in standard modes. In the latter, the flat neck is ruptured closer to the larger head associated with the heavy fragment in order to produce fragments close to mass symmetry. As a result, the heavy fragment is formed with a smaller deformation in contrast to its more deformed partner. Even at the symmetric division, the complementary fragments in standard modes are formed with much different deformations on the basis of the multi-modal fission model. As a result, a saw-tooth structure is expected to be observed in the angular momentum as a function of fragment mass. On the other hand, due to the symmetric precission shapes in the SL mode, the deformation and angular momentum of a fragment is expected to increase with its mass as seen in Figure 2. The behavior of the average angular momentum as a function of mass weighted over the fission modes is also shown in the same figure. The structure on this curve carries the signatures of both mode probabilities and angular momenta. For example, the sharp drop around $A \cong 122$ for ²³⁵U(n_{th}, f) is a result of the diminishing contribution of the SL mode to the yield distribution as one moves away from the symmetric split. The location and degree of sharpness is due to the contribution of S1 to the symmetric region. Experimental data on the angular momentum distribution around this region would be very valuable. It has been shown¹⁶ that the multi-modal fission model may be capable of explaining the experimental results on isomer ratios.

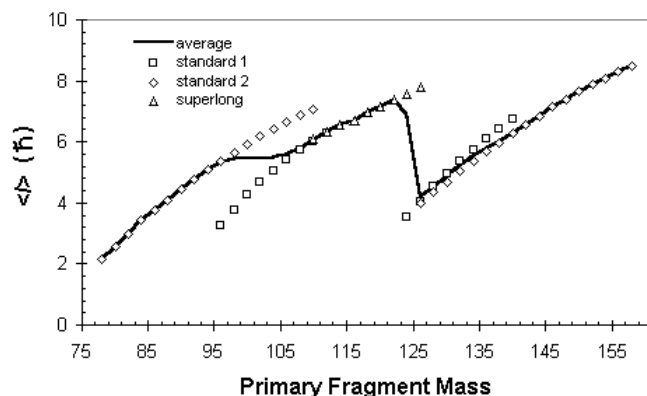


Figure 2. The dependence of calculated average angular momentum on fragment mass for fission modes in ²³⁵U(n_{th}, f).

The angular momentum of fission fragments due to the bending motion may be altered due to their Coulomb excitation. There may be an increase or decrease in this angular momentum. In the calculations of Dietrich and Zielinska-Pfabe⁸ an increase of about 10–15% was concluded for this effect. Mişicu et al.¹⁷ concluded that the Coulomb excitation accounts less than 10% of the final spin of fragments in the cold fission of ²⁵²Cf. A simple classical model⁶ has been proposed to investigate the change in the distribution of angular momenta due to the subsequent Coulomb excitation. In this model, it is assumed that the shape of fragments do not change during acceleration. As a result, the axially symmetric fragment with intrinsic quadrupole moment feels a torque depending on the time it takes to rotate it, and changes its angular momentum by ΔI . The angular momentum due to Coulomb excitation is assumed to be perpendicular to the angular momentum due to the bending motion. The results of our calculations within this model indicated that the post-scission change of the fragment angular momenta is relatively small (only a small fraction of \hbar). This result may easily be understood because the aligned configuration for primary fission fragments is the most probable scission condition in which the torque felt by each fragment vanishes. It may be deduced from the values that angular momentum change due to Coulomb excitation is negligible with the assumption that it is perpendicular to the angular momentum due to the bending motion. However, detailed trajectory calculations are needed to make a final decision about the quantity of this effect.

In Figure 3, our calculated values of the average angular momenta are compared with the experimental results³ for thermal neutron-induced fission of ²³⁵U. The preliminary conclusion reached by Shannon³ in his measurements of the ratio of average spins at which discrete states are populated in cold fission to the average when the same nucleus is formed as a primary product in fission events in which the total number of prompt neutrons is equal to four. The value of this ratio suggests that the average angular momentum of primary fragments is only about $1\hbar$ higher than in cold fission fragments. The $1\hbar$ may be taken to be arising from the reduction in the angular momentum due to two neutrons on the average being emitted from each primary fragment. Calculation with the statistical evaporation code CASCADE¹⁸ suggesting that each neutron evaporation reduces the average entry point spin by $\approx 0.5\hbar$ is consistent with this above conclusion. CASCADE calculations also suggest that statistical γ transitions are expected to produce an even smaller reduction in the entry point spins. Shannon, considering effects of neutron and statistical γ ray emission in the angular momentum, corrected the angular momentum of fission products to obtain that of primary fission fragments.³ They are given in Figure 3. The agreement is observed between our calculated values within the BGM model and the experimental values of the average angular momenta as a function of fission fragment masses.

The effect of intrinsic excitation energy on the angular mo-

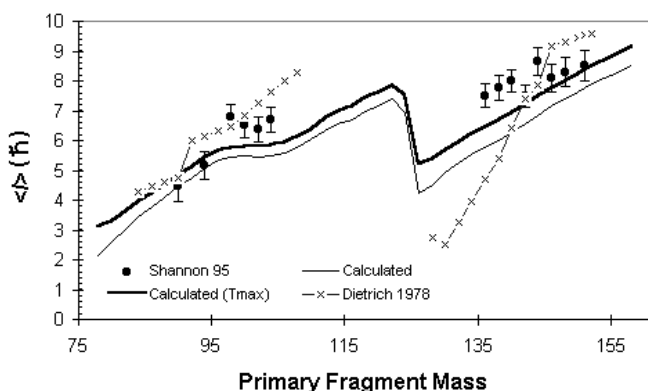


Figure 3. A comparison of calculated and experimental average angular momentum as a function of fragment mass in ²³⁵U(*n*_{th}, *f*).

mentum distribution was examined. The precission shape parameters were determined for the nuclear temperature T_i for the *i*-th mode with the intrinsic excitation energy at scission E_{si}^* . The latter energy was taken to be 26% of the potential energy freed on descent from the last barrier before scission ΔU_i for ²³⁵U(*n*_{th}, *f*). The nuclear temperatures obtained in this way were close to 0.4 MeV. The curve indicated as the calculated values of the average angular momenta in Figure 3 was for $T = 0.4$ MeV which was almost indistinguishable from the corresponding one for $T = 0$. Assuming ΔU_i is fully converted into intrinsic excitation energy, a nuclear temperature of about 0.8 MeV would be expected. The thicker curve in Figure 3 represents $T = 0.8$ MeV. Such an approximation gives an upper limit of the effect of temperature on angular momenta since it leaves no room for precission kinetic energy, and energy for other degrees of collective excitations other than deformation.

Figure 3 also shows the results of the calculations made by Dietrich and Zielinska-Pfabe⁸ for the zero temperature case. In their work, the fissioning system at the scission point was represented as two nuclei with quadrupole deformations that were obtained by the total excitation energies of the fragments. Their theoretical results were in good agreement with the γ -ray multiplicity experiment¹ under the assumption that the angular momentum of a fission fragment is approximately equal to twice the number of γ rays, $N(A)_\gamma$. They suggested that there are weak points in the approximate relation $\bar{l}_i = 2N_\gamma$. Since the character of the γ -ray cascade is expected to depend on the nuclear structure of the fragments such a simple relation may not be realistic. As seen in Figure 3, contrary to the close relation between our results and the recent experimental data, the results of Dietrich and Zielinska-Pfabe are unsatisfactory especially for the heavy fragments. This may be because the scission configuration is represented better in the multi-modal fission model used in our study.

In addition, the average angular momentum of primary fission fragments over all modes and masses were calculated and found to be $5.7\hbar$ for ²³⁵U(*n*_{th}, *f*). The average angular momentum of primary fission products, obtained by Ahmad and Phillips¹⁹ is equal to $4.6\hbar$ for the ²³⁵U(*n*_{th}, *f*). The difference of $1.1\hbar$ between the angular momenta of primary fission fragments and products is consistent with our estimation of the decrease in angular momentum due to prompt neutron and statistical γ -ray emissions.

Average angular momentum values are also calculated for ²⁵²Cf(sf) and ²⁴⁸Cm(sf). Reasonable agreement with experimental data has been obtained for these systems.

Acknowledgement. Financial support of METU through AFP 94-01-03-05 and AFP 96-01-03-06 are gratefully acknowledged.

References

- (1) F. Pleasonton, R. L. Ferguson, and H. W. Schmitt, Phys. Rev. C **6**, 1023 (1972).
- (2) J. B. Wilhelmy, E. Cheifetz, R. C. Jared, S. G. Thompson, H. R. Bowman, and J. O. Rasmussen, Phys. Rev. C **5**, 2041 (1972).
- (3) J. A. Shannon, Thesis, University of Manchester, 1995.
- (4) Y. S. Abdelrahman, J. L. Durell, W. Galletly, W. R. Phillips, I. Ahmad, R. Holzmann, R. V. F. Janssens, T. L. Khoo, W. C. Ma, and M. W. Drigert, Phys. Lett. B **199**, 504 (1987).
- (5) G. M. Ter-Akopian, J. H. Hamilton, Yu. Ts. Oganessian, A. V. Daniel, J. Kormicki, A. V. Ramayya, G. S. Popeko, B. R. S. Babu, Q.-H. Lu, K. Butler-Moore, W.-C. Ma, E. F. Jones, J. K. Deng, D. Shi, J. Kliman, M. Morhac, J. D. Cole, R. Aryaeinejad, N. R. Johnson, I. Y. Lee, and F. K. McGowan, Phys. Rev. C **55**, 1146 (1997).
- (6) J. O. Rasmussen, W. Nörenberg, and H. J. Mang, Nucl. Phys. A **136**, 465 (1969).

- (7) M. Zielinska-Pfabe and K. Dietrich, *Phys. Lett.* **49B**, 123 (1974).
- (8) K. Dietrich and M. Zielinska-Pfabe, *Theory of the Angular Momentum Distribution of Fission Fragments* (private communication, 1978).
- (9) J. O. Rasmussen, S. Y. Chu, D. Strellis, R. Donangelo, L. F. Canto, Y. X. Dardenne, J. D. Cole, M. A. Stoyer, and J. H. Hamilton, *Dynamical Aspects of Nuclear Fission, Dubna, 1996*, p. 289.
- (10) U. Brosa, S. Grossmann, and A. Müller, *Phys. Rep.* **197**, 167 (1990).
- (11) T. Fan, J. Hu, and S. Bao, *Nucl. Phys. A* **591**, 161 (1995).
- (12) J. R. Nix and W. Swiatecki, *Nucl. Phys.* **71**, 1 (1965).
- (13) J. Blocki, J. Randrup, W. J. Swiatecki, and C. F. Tsang, *Ann. Phys. (NY)* **105**, 427 (1977).
- (14) A. C. Wahl, *J. Radioanal. Chem.* **55**, 111 (1980); A. C. Wahl, *At. Data Nucl. Data Tables* **39**, 1 (1988).
- (15) A. Wolf and E. Cheifetz, *Phys. Rev. C* **13**, 1952 (1976).
- (16) M. Kildir, Z. Mörel, Z. Büyükmumcu, and H. N. Erten, *J. Radioanal. Nucl. Chem.* **221**, 161 (1997).
- (17) Ş. Mişicu, A. Sandulescu, G. M. Ter-Akopian, and W. Greiner, *Phys. Rev. C* **60**, 034613 (1999).
- (18) F. Pühlhofer, *Nucl. Phys. A* **280**, 267 (1977).
- (19) I. Ahmad and W. R. Phillips, *Rep. Prog. Phys.* **58**, 1415 (1995).